Int. J. Solids Structures, 1974, Vol. 10, pp. 1417–1429. Pergamon Press. Printed in Gt. Britain.

EFFECTS OF INPLANE CONSTRAINTS AND CURVATURE ON COMPOSITE PLATE BEHAVIOR

R. C. FORTIER

Southeastern Massachusetts University, North Dartmouth, Massachusetts U.S.A.

and

J. N. ROSSETTOS

Northeastern University, Boston, Massachusetts 02115, U.S.A.

(*Received* 19 *November* 1973; *revised* 9 *April* 1974)

Abstract—An investigation into the behavior of unsymmetrically laminated anisotropic plates is carried out. Using the basic assumptions of linear plate theory and strain–displacement relations modified to account for small initial curvature, energy formulations are established and the Ritz method utilized to obtain solutions for static deflections and natural frequencies of vibration. The boundary condition with particular inplane restraints and the particular stacking arrangement are shown to have important effects on plate response when bending–extensional coupling is present. Small initial curvature is shown to greatly increase natural frequencies and may obscure the effects of bending–extensional coupling due to nonsymmetrical layering. The increase in lateral stiffness due to curvature is also shown to depend heavily on fiber orientation, orthotropicity and boundary conditions.

NOTATION

A_{ij}, B_{ij}, D_{ij}	constitutive coefficients defined by equation (5)
a, b	plate dimensions along x, y axes respectively
B	inertia matrix defined by equation (19)
E_{ij}, F_{ij}, G_{ij}	coefficients for displacements u^0, v^0 and w respectively
E_{11}, E_{22}	principal Young's moduli in plate 1 and 2 directions respectively
f	load vector defined by equation (16)
G_{12}	shear moduli in 1–2 plane
h_k	distance from midplane to lamina boundary as shown in Fig. 1
h	total plate thickness
K	stiffness matrix defined by equation (13)
M_x, M_y	bending moments per unit length on plate sections perpendicular to x and y axes respectively
N	number of layers in plate
N_x, N_y	normal forces per unit length on plate sections perpendicular to the x and y axes respectively
N_{xy}	shearing force per unit length on plate section perpendicular to the x or y axes
Q	potential energy due to transverse loading
Q_{ij}	constitutive coefficients for orthotropic lamina
q	intensity of transverse loading
T	kinetic energy
U	strain energy
u^0, v^0	tangential displacements of the midplane in the x and y directions respectively
w	displacement normal to the midplane
w_0	initial shape of the plate
x	displacement vector given by equation (15)
γ_{xy}	shearing strain
δ	maximum amount of initial curvature as shown in Fig. 2
$\varepsilon_x, \varepsilon_y$	normal strains in x and y directions respectively
$\theta_{ui}, \theta_{vi}, \theta_{wi}$	displacement functions for u^0, v^0 and w displacements respectively, which satisfy geometric boundary conditions at $y = 0$ and $y = b$

λ	frequency parameter
ν_{12}	Poisson's ratio
Π	total system energy
ρ	mass per unit volume
σ_x, σ_y	normal stress components in x and y directions respectively
τ_{xy}	shearing stress
ϕ_{ui}, ϕ_{vi}, ϕ_{wi}	displacement functions for u^0, v^0 and w displacements respectively which satisfy geometric boundary conditions at $x = 0$ and $x = a$
ω	natural frequency.

INTRODUCTION

In recent years there has been a significant increase in the interest given fiber reinforced laminated composite materials due mainly to their high strength-to-weight ratios and to the degree of design flexibility their usage permits. For cases in which the individual laminae are unsymmetrically layered about the geometric midplane in either material properties or principal axis orientation, significant departure from homogeneous plate behavior results. In this regard Reissner and Stavsky[1] are credited with first demonstrating the existence of a linear coupling between the transverse bending and inplane stretching modes not found in homogeneous media. Later Yang *et al.*[2] formulated a laminated plate theory again showing the existence of bending–extensional coupling for a more general class of laminates, however, no solutions were presented for the nonsymmetrical case.

Whitney and Leissa[3] extended composite material analysis by a derivation resulting in three equations of motion cast in terms of the three orthogonal displacements. The boundary conditions assumed so as to obtain closed form solutions were hinges allowing inplane displacements tangent to the boundary for the angle-ply case and inplane displacements normal to the boundary for the cross-ply case. Also investigated by these authors[4] was a simply-supported plate with no inplane restraints in either tangential or normal directions. A Fourier series technique was used to approximately solve the stress function and displacement equations. In both these investigations, solutions for angle-ply and cross-ply configurations showed that the presence of coupling reduces plate stiffness which in turn increases static deflections and reduces natural frequencies and critical loads. Coupling was shown to be a function of the number of layers and their degree of anistropy. Whitney's examination [5] of fully restrained layered plates, using a Fourier series technique to approximately solve the displacement equations showed the same qualitative results regarding the nature and causes of coupling.

In this paper the behavior of the unsymmetric angle-ply and cross-ply plates with and without small initial curvature is investigated. As a result of bending–extensional coupling, the usual simply supported and clamped boundaries must be more explicitly identified by prescribing either inplane displacements or forces. Hence four types of edge conditions are considered for both angle-ply and cross-ply configurations, namely three hinge conditions and a fully restrained condition, so as to ascertain the effects of this parameter on plate response. As the results will show, a wide variation in the severity of bending–extensional coupling occurs depending on the particular boundary condition (the type of inplane restraint is critical) and ply configuration. Bending–extensional coupling due to the presence of initial curvature, in contrast to that due to unsymmetric layering, produces a stiffening of the plate. The counteracting effects from the two coupling sources is investigated here to determine the ranges of predominance and the combined effect on natural frequencies.

Results show that a very slight amount of curvature may produce large frequency increases which tend to predominate over the bending–extensional coupling effects from nonsymmetry.

FORMULATION OF THE GOVERNING EQUATIONS

A conventional x, y, z coordinate system, as shown in Fig. 1, is used to identify the plate geometry, with distances to the individual laminae being measured from the geometrical midplane. The Ritz method requires the total system energy expressed in terms of the displacements. To this end the strain energy due to bending for the plane stress situation assumed here is

$$U = \int_V (\sigma_x \varepsilon_x + \sigma_y \varepsilon_y + \tau_{xy} \gamma_{xy})\, dV. \tag{1}$$

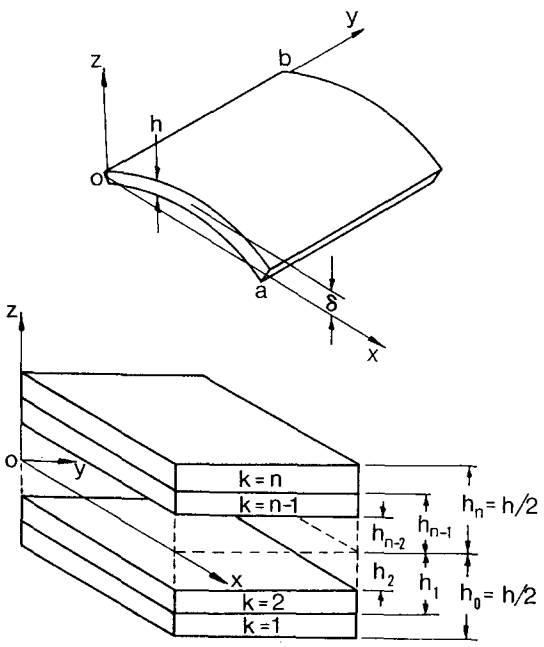

Fig. 1. Single constant curvature representation and lamina indentification.

The usual assumptions of linear shallow shell theory[6] leads to the following strain–displacement expressions

$$\begin{aligned} \varepsilon_x &= u^0{}_{,x} - w w_{0,xx} - z w_{,xx} \\ \varepsilon_y &= v^0{}_{,y} - w w_{0,yy} - z w_{,yy} \\ \varepsilon_{xy} &= u^0{}_{,y} + v^0{}_{,x} - 2 w w_{0,xy} - 2 z w_{,xy} \end{aligned} \tag{2}$$

where u^0 and v^0 are the tangential displacements of the midplane in the x and y directions respectively, w is the displacement normal to the midplane in the z direction and w_0 represents the initial shape of the plate. Commas denote differentiation with respect to the subscripted variables.

For the kth orthotropic laminae of the plate, the generalized Hooke's law is expressed as

$$\begin{bmatrix} \sigma_x^{(k)} \\ \sigma_y^{(k)} \\ \tau_{xy}^{(k)} \end{bmatrix} = \begin{bmatrix} Q_{11}^{(k)} & Q_{12}^{(k)} & Q_{16}^{(k)} \\ Q_{12}^{(k)} & Q_{22}^{(k)} & Q_{26}^{(k)} \\ Q_{16}^{(k)} & Q_{26}^{(k)} & Q_{66}^{(k)} \end{bmatrix} \begin{bmatrix} \varepsilon_x \\ \varepsilon_y \\ \gamma_{xy} \end{bmatrix} \tag{3}$$

where the $Q_{ij}^{(k)}$ are related to the familiar engineering constants as shown in [7]. Separating (1) into piecewise integration through the thickness of the n-layered plate and using relations (2) and (3), the expression for strain energy due to bending in terms of displacements u^0, v^0 and w and the initial shape, w_0, is given by

$$\begin{aligned} U = \frac{1}{2}\int_0^a \int_0^b \{ & A_{11}(u^0{}_{,x} - ww_{0,xx})^2 \\ & + 2A_{12}(u^0{}_{,x} - ww_{0,xx})(v^0{}_{,y} - ww_{0,yy}) \\ & + 2A_{16}(u^0{}_{,x} - ww_{0,xx})(u^0{}_{,y} + v^0{}_{,x} - 2ww_{0,xy}) \\ & + A_{22}(v^0{}_{,y} - ww_{0,yy})^2 \\ & + 2A_{26}(v^0{}_{,y} - ww_{0,yy})(u^0{}_{,y} + v^0{}_{,x} - 2ww_{0,xy}) \\ & + A_{66}(yu^0{}_{,y} + v^0{}_{,x} - 2ww_{0,xy})^2 \\ & - 2B_{11}(u^0{}_{,x} - ww_{0,xx})w_{,xx} \\ & - 2B_{12}[(u^0{}_{,x} - ww_{0,xx})w_{,yy} + (v^0{}_{,y} - ww_{0,yy})w_{,xx}] \\ & - 2B_{16}[2(u^0{}_{,x} - ww_{0,xx})w_{,xy} + (u^0{}_{,y} + v^0{}_{,x} - 2ww_{0,xy})w_{,xx}] \\ & - 2B_{22}(v^0{}_{,y} - ww_{0,yy})w_{,yy} \\ & - 2B_{26}[2(v^0{}_{,y} - ww_{0,yy})w_{,xy} + (u^0{}_{,y} + v^0{}_{,x} - 2ww_{0,xy})w_{,yy}] \\ & - 4B_{66}(u^0{}_{,y} + v^0{}_{,x} - 2ww_{0,xy})w_{,xy} \\ & + D_{11}w^2{}_{,xx} + 2D_{12}\,w_{,xx}\,w_{,yy} + 4D_{16}\,w_{,xx}\,w_{,xy} \\ & + D_{22}\,w^2{}_{,yy} + 4D_{26}\,w_{,yy}\,w_{,xy} + 4D_{66}\,w^2{}_{,xy}\}\,\mathrm{d}x\,\mathrm{d}y \end{aligned} \tag{4}$$

where the limits a and b are the plate dimensions in the x and y directions respectively, and where

$$(A_{ij},\, B_{ij},\, D_{ij}) = \sum_{k=1}^{n} \int_{h_k}^{h_{k-1}} Q_{ij}^{(k)}(1,\, z,\, z^2)\,\mathrm{d}z. \tag{5}$$

The contribution to the total system energy from a transversely applied load is equal to

$$Q = -\int_0^a \int_0^b qw\,\mathrm{d}x\,\mathrm{d}y \tag{6}$$

where Q is the potential energy and $q(x, y)$ is the load per unit area. The kinetic energy T, is given by

$$T = \frac{1}{2}\int_0^a \int_0^b \rho h[(u^0{}_{,t})^2 + (v^0{}_{,t})^2 + (w_{,t})^2]\,\mathrm{d}x\,\mathrm{d}y \tag{7}$$

where ρ is the mass per unit volume and h is the total plate thickness.

In order to employ the Ritz procedure, use must be made of either the theorem of stationary potential energy for static analysis or Hamilton's principle for dynamic analysis, which for a conservative system are given respectively by

$$\delta(U + Q) = 0 \tag{8}$$

and

$$\delta(U - T) = 0. \tag{9}$$

In addition, the functions assumed for the displacement will take the following form

$$w = \sum_{i=1}^{m} \sum_{j=1}^{n} E_{ij}\, \phi_{wi}(x)\theta_{wj}(y)$$

$$u^0 = \sum_{i=1}^{p} \sum_{j=1}^{q} F_{ij}\, \phi_{ui}(x)\theta_{uj}(y)$$

$$v^0 = \sum_{i=1}^{r} \sum_{j=1}^{s} G_{ij}\, \phi_{vi}(x)\theta_{vj}(y) \tag{10}$$

where $\phi(x)$ and $\theta(y)$ are suitable functions satisfying the geometric boundary conditions along $x = 0, a$ and $y = 0, b$ respectively, and E_{ij}, F_{ij} and G_{ij} are undetermined coefficients.

Designating the total system energy as Π, then since $\Pi = \Pi(u^0, v^0, w)$ and u^0, v^0 and w are functions of the undetermined coefficients E_{ij}, F_{ij} and G_{ij}, the variational problem may be replaced by the equivalent problem of finding the minimum of Π with respect to the coefficients. Accordingly, we may write

$$\frac{\partial \Pi}{\partial(E_{kl}, F_{kl}, G_{kl})} = 0 \tag{11}$$

where $k = 1, \ldots, m$ and $l = 1, \ldots, n$. Assume for the moment that Π is composed of all the energy terms considered, i.e. $\Pi = U + Q - T$ noting that for the static case $T = 0$ and for the free vibration case $Q = 0$. If expressions (4, 6, 7 and 10) are now substituted into equation (11) and the differentiation carried out, there results a system of $m \cdot n + p \cdot q + r \cdot s$ algebraic equations in the coefficients E_{kl}, F_{kl}, and G_{kl}. For the static deflection problem, these equations may be written as

$$[K]\{x\} = \{f\} \tag{12}$$

where K is the stiffness matrix given by

$$[K] = \begin{bmatrix} K^{11}_{1111} \cdots K^{11}_{mn11} & K^{12}_{1111} \cdots K^{12}_{mn11} & K^{13}_{1111} \cdots K^{13}_{mn11} \\ \vdots \quad \ddots \quad \vdots & \vdots \quad\quad \vdots & \vdots \quad\quad \vdots \\ K^{11}_{mnmn} & K^{12}_{11mn} \cdots K^{12}_{mnmn} & K^{13}_{11mn} \cdots K^{13}_{mnmn} \\ & K^{22}_{1111} \quad K^{22}_{mn11} & K^{23}_{1111} \quad K^{23}_{mn11} \\ \text{symmetric} & \quad\quad \ddots \quad\quad \vdots & \vdots \quad\quad \vdots \\ & K^{22}_{mnmn} & K^{23}_{11mn} \cdots K^{23}_{mnmn} \\ & & K^{33}_{1111} \cdots K^{33}_{mn11} \\ & & \quad\quad \ddots \quad\quad \vdots \\ & & K^{33}_{mnmn} \end{bmatrix}. \tag{13}$$

For a single constant curvature of quadratic representation

$$w_0 = 4\delta(x/a - x^2/a^2) \tag{14}$$

where δ represents the maximum initial rise, the elements of K are given in the Appendix. The displacement vector x is given by

$$\{x\}^T = \{E_{11}, E_{12} \ldots, E_{mn}, F_{11}, F_{12}, \ldots, F_{mn}, G_{11}, G_{12}, \ldots, G_{mn}\} \tag{15}$$

where E_{ij}, F_{ij} and G_{ij} are the displacement coefficients of equation (10). The load vector f is given by

$$\{f\}^T = \{f_{11}, f_{12}, \ldots, f_{mn}, 0, 0, \ldots, 0\} \tag{16}$$

where

$$f_{kl} = \int_0^a \int_0^b q\phi_{wk}\theta_{wl}\,\mathrm{d}x\,\mathrm{d}y. \tag{17}$$

The free vibration problem may be written as

$$[B^{-1}K - \lambda I]\{x\} = \{0\} \tag{18}$$

where B is the diagonal inertia matrix given by

$$\begin{aligned}[B] = \Bigg[& \int_0^a \int_0^b \phi_{w1}\phi_{w1}\theta_{w1}\theta_{w1}\,\mathrm{d}x\,\mathrm{d}y, \ldots, \int_0^a \int_0^b \phi_{wm}\phi_{wn}\theta_{wm}\theta_{wn}\,\mathrm{d}x\,\mathrm{d}y, \\ & \int_0^a \int_0^b \phi_{u1}\phi_{u1}\theta_{u1}\theta_{u1}\,\mathrm{d}x\,\mathrm{d}y, \ldots, \int_0^a \int_0^b \phi_{um}\phi_{un}\theta_{um}\theta_{un}\,\mathrm{d}x\,\mathrm{d}y, \\ & \int_0^a \int_0^b \phi_{v1}\phi_{v1}\theta_{v1}\theta_{v1}\,\mathrm{d}x\,\mathrm{d}y, \ldots, \int_0^a \int_0^b \phi_{vm}\phi_{vn}\theta_{vm}\theta_{vn}\,\mathrm{d}x\,\mathrm{d}y \Bigg]\end{aligned} \tag{19}$$

I is the identity matrix and $\lambda = \rho h\omega^2$ where ω is the natural frequency.

It can be observed from expressions (13) and (15) that the submatrices K^{ij} have an important physical interpretation. Bending–extensional coupling arising from the presence of initial curvature and/or unsymmetrical layering of the laminae is represented by the off-diagonal submatrices K^{12}, K^{13} and K^{23}. Specifically K^{12} represents coupling between the u^0 and w displacements, K^{13} represents coupling between v^0 and w and K^{23} represents coupling between u^0 and v^0. The amount of coupling then depends on the magnitude of the elements of these submatrices which, by the formulations in the Appendix, are shown to be functions of the constitutive coefficients A_{ij} and B_{ij}, the amount of curvature δ and the particular choice of the functions $\phi(x)$ and $\theta(y)$.

BOUNDARY CONDITIONS AND DISPLACEMENT FUNCTIONS

The four boundary conditions are now specified and in addition, functions will be chosen so as to model the displacements in accordance with equation (10). The first boundary assumed is designated HFT for hinge-free-tangential in which we have

$$\begin{aligned} w = u^0 = M_x = N_{xy} = 0 \quad &\text{at} \quad x = 0, a \\ w = v^0 = M_y = N_{xy} = 0 \quad &\text{at} \quad y = 0, b \end{aligned} \tag{20}$$

and for which the following displacement functions are assumed

$$\begin{aligned} \phi_{wi} = \phi_{ui} &= \sin i\pi x/a, \qquad \phi_{vi} = \cos i\pi x/a \\ \theta_{mj} = \theta_{vj} &= \sin j\pi y/b, \qquad \theta_{uj} = \cos j\pi y/b. \end{aligned} \tag{21}$$

The second boundary, designated HFN for hinge-free-normal, is described by

$$\begin{aligned} w = v^0 = M_x = N_x = 0 \quad &\text{at} \quad x = 0, a \\ w = u^0 = M_y = N_y = 0 \quad &\text{at} \quad y = 0, b \end{aligned} \tag{22}$$

for which the following functions are assumed

$$\begin{aligned} \phi_{wi} = \phi_{vi} &= \sin i\pi x/a, \qquad \phi_{ui} = \cos i\pi x/a \\ \theta_{wj} = \theta_{uj} &= \sin j\pi y/b, \qquad \theta_{vi} = \cos j\pi y/b. \end{aligned} \tag{23}$$

The third boundary, designated HR for hinge-restrained, is described by

$$\begin{aligned} w = u^0 = v^0 = M_x = 0 \quad &\text{at} \quad x = 0, a \\ w = u^0 = v^0 = M_y = 0 \quad &\text{at} \quad y = 0, b \end{aligned} \tag{24}$$

for which the following displacement functions are assumed

$$\begin{aligned} \phi_{wi} = \phi_{ui} = \phi_{vi} &= \sin i\pi x/a \\ \theta_{wj} = \theta_{uj} = \theta_{vj} &= \sin j\pi y/b. \end{aligned} \tag{25}$$

The fourth boundary, designated CL for clamped, is described by

$$\begin{aligned} w = w_{,x} = u^0 = v^0 = 0 \quad &\text{at} \quad x = 0, a \\ w = w_{,y} = u^0 = v^0 = 0 \quad &\text{at} \quad y = 0, b \end{aligned} \tag{26}$$

for which the following displacement functions are assumed

$$\begin{aligned} \phi_{wi} &= \cosh \beta_i x - \cos \beta_i x - \alpha_i(\sinh \beta_i x - \sin \beta_i x) \\ \phi_{ui} = \phi_{vi} &= \sin i\pi x/a \\ \theta_{wj} &= \cosh \beta_j y - \cos \beta_j y - \alpha_j(\sinh \beta_j y - \sin \beta_j y) \\ \theta_{uj} = \theta_{vj} &= \sin j\pi y/b \end{aligned} \tag{27}$$

where α and β are characteristic functions corresponding to the mode shapes of a vibrating beam and tabulated in[8]. Similar functions were used to study the free vibration of flat, clamped anisotropic plates in[9].

ACCURACY AND CONVERGENCE

As the number of terms in the assumed displacement function series is increased, the Ritz method will generate solutions which will in the limit converge to the exact solution. An important question then is what degree of convergence has been achieved for any given number of terms. As previously noted, boundary conditions (20) are exactly satisfied by (21) for the angle-ply configuration, and boundary conditions (22) are exactly satisfied by (23) for the cross-ply configuration. These results have been formulated in[3] and served as excellent checks on the accuracy of the Ritz method results. Five term displacement function series, i.e. $m = n = p = q = r = s = 5$ in expressions (10), were assumed and agreement was shown to be excellent, the greatest difference being one digit in the fourth decimal place.

The fundamental frequency of a CL two-layered angle-ply was compared to the results given by Whitney[5] and the largest difference between the two for any fiber angle was two digits in the third decimal place. Since the Fourier series method employed by Whitney was

not exact, the very similar results should lend credibility to both results. Curved plate results were checked with isotropic plate results from the literature[10] and agreement for the four lowest frequencies was to a minimum of three significant figures. Acceptable convergence of solutions, investigated by increasing the number of terms in the displacement function series and observing the asymptotic nature of the results, was achieved for both frequency and static deflection cases. The worst case occurred for the two-layered CL boundary solution in which the fundamental frequency converged to within 0·40 per cent and the fourth lowest frequency to within 3·3 per cent. Static deflection convergence for this case was to within 1·2 and 0·50 per cent for the two-layered and infinite-layered cases respectively.

DISCUSSION AND RESULTS

The effect of boundary conditions on the stiffness of flat angle-ply and cross-ply composites is shown in Figs. 2 and 3 respectively. Note that the filament angle θ is measured from the x axis in all the cases presented. Clearly the type of boundary condition, and in particular the type of inplane restraint for the three hinge cases, plays a significant role in the determination of plate behavior when bending–extensional coupling is present. In addition there are pronounced differences in behavior between the cross-ply and angle-ply configurations under identical boundary conditions. This is indicated in Figs. 2 and 3 by the reversal of relative positions for the HFN and HFT cases in so far as the degree of stiffness present. For

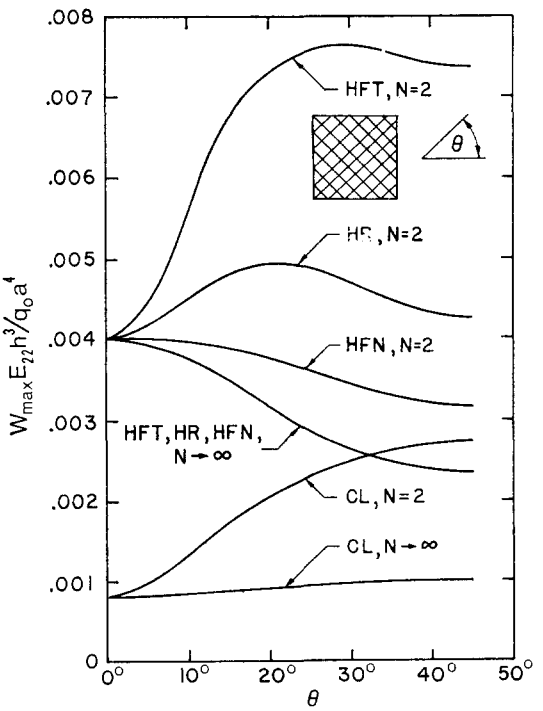

Fig. 2. Maximum deflection as a function of fiber orientation and boundary conditions for a square angle-ply plate under uniform transverse loading ($E_{11}/E_{22} = 40, G_{12}/E_{22} = 1, \nu_{12} = 0{\cdot}25$, N = no. of layers).

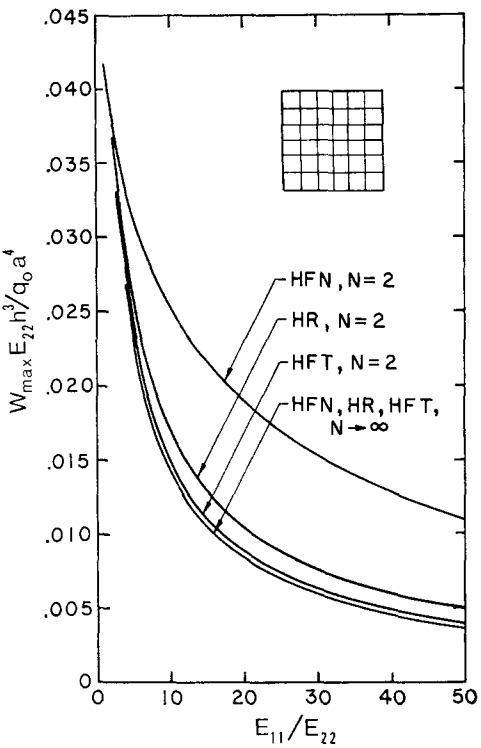

Fig. 3. Maximum deflection as a function of the degree of anisotropy and boundary conditions for a square cross-ply plate under uniform transverse loading ($G_{12}/E_{22} = 0{\cdot}50$, $\nu_{12} = 0{\cdot}25$, N = no. of layers).

example, Fig. 2 shows that for an angle-ply, the HFT two-layered case is the least stiff for any non-zero θ, indicating a large degree of bending–extensional coupling is present. Figure 3, however, shows that for a cross-ply, the HFT two-layered case is the stiffest for any degree of orthotropicity, and in fact differs only slightly from the $N \to \infty$ case in which bending–extensional coupling is not present. Note is made of the fact that all three hinge boundary conditions produce the same results for the infinite-layered solution. This results from the fact that the only difference in these three conditions is in the inplane displacements allowed along the boundary. For the infinite-layered case the bending and extensional modes are uncoupled and as a result the solution to the bending problem requires only the restraints on the transverse displacement, and these being equal for all three hinges, the infinite-layered solutions coincide.

Prior to this investigation it has been suggested by Whitney and Leissa[4] and by Whitney [5] that the solution to coupled plate problems may be relatively insensitive to the type of inplane boundary conditions. Their findings suggest the use of the so called "reduced bending stiffness method", which in effect neglects inplane conditions, as a viable means of solution for cross-ply plates, while they note some discrepancy in results for certain orientations of angle-ply plates. As results here show, however, solutions are indeed sensitive to inplane boundary conditions for both cross-ply and angle-ply configurations and, as a result, the use of the reduced bending stiffness method is discouraged.

When a transverse displacement occurs in an initially curved plate, the greatest stretching occurs in the circumferential direction. If normal inplane displacements are precluded at the boundary, as in the HFT, HR and CL cases, there results an increase in stiffness and hence in natural frequencies. Figure 4 shows a comparison of the effect small curvature has on natural frequency for the HFT and HFN cases. For an equivalent flat plate both the infinite-layered cases start at a nondimensional frequency of approx 19 at $\theta = 0°$, go to a maximum of approx 25 at $\theta = 45°$ and return symmetrically to 19 at $\theta = 90°$. In the presence of small initial curvature (a rise to length ratio of 0·01) the HFT case shows a great increase in frequency when $\theta = 0°$ since in this orientation the greatest amount of stretching occurs in

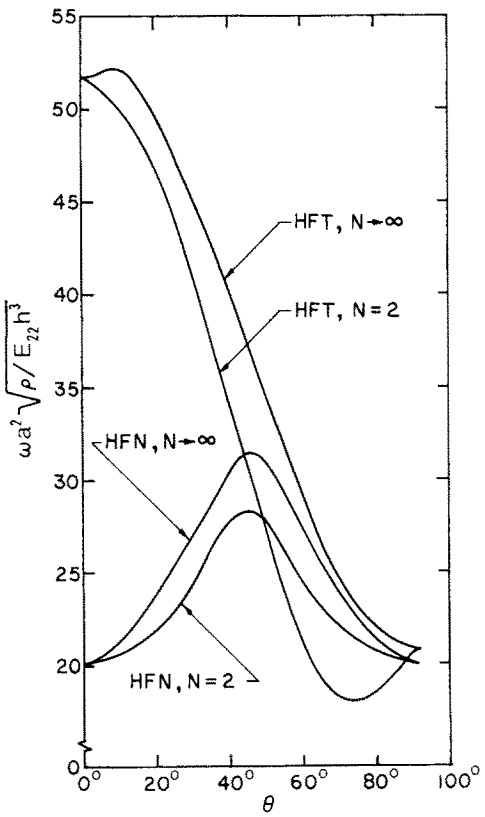

Fig. 4. Fundamental frequency as a function of fiber orientation and boundary conditions for a square angle-ply plate with small initial curvature $E_{11}/E_{22} = 40$, $G_{12}/E_{22} = 1$, $\nu_{12} = 0{\cdot}25$, $\delta/a = 0{\cdot}01$, $N =$ no. of layers).

the direction of maximum stiffness and moreover the normal inplane displacements are restrained. For the HFN boundary condition, since normal inplane displacements are allowed, the effect of curvature is considerably lessened.

Figure 5 shows the effect of small initial curvature on the fundamental frequency for the limiting case of infinite layers for each of the four boundary conditions considered. In the presence of curvature these solutions no longer coincide as they did for the flat plate case since while coupling due to non-symmetrical layering is eliminated, there is additional coupling due to the curvature and hence the boundary condition affects plate response. Of

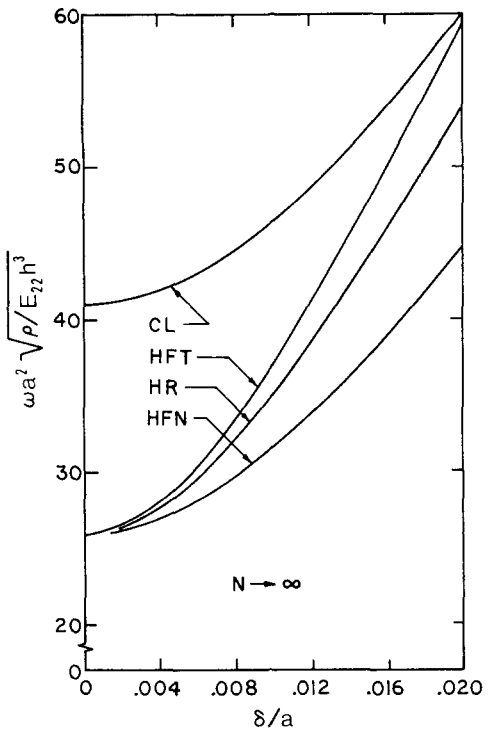

Fig. 5. Fundamental frequency as a function of initial curvature and boundary conditions for a square 45° angle-ply plate ($E_{11}/E_{22} = 40$, $G_{12}/E_{22} = 1$, $\nu_{12} = 0{\cdot}25$, $N \to \infty$).

the three hinge boundaries considered, the HFN case since it alone allows inplane motion normal to the boundary, shows the least stiffening effect due to the curvature. Interestingly, the CL case appears less affected than the remaining two hinge cases.

When the plate is flat the difference between the two-layered and infinite-layered solutions for any boundary condition is due to the amount of bending–stretching coupling present in the two-layered case, its effect being a reduction in stiffness and hence in frequency. Introducing small curvature produces a frequency change which, as shown in Fig. 6, for an angle-ply can obscure and in fact completely predominate the coupling effects due to nonsymmetrical layering. As the curvature increases, this effect becomes progressively more pronounced. One may be inclined to conclude that for plates of greater curvature than $\delta/a = 0{\cdot}02$ the effect on stiffness due to coupling from nonsymmetrical layering is negligible. This may indeed be the case, and numerical results for δ/a in the range of 0·05 to 0·10 could substantiate this. However, this converging behavior was not noted for a cross-ply with $\delta/a \leq 0{\cdot}02$ since the second mode frequency intersected the first mode within this range and produced a larger frequency difference at $\delta/a = 0{\cdot}02$ than at $\delta/a = 0$.

Taking all the results together it should be clear that the amount of stiffening due to curvature will depend heavily on fiber orientation, orthotropicity and boundary conditions. Results were also obtained for higher mode frequencies and are given in[11]. Generally they show trends similar to the fundamental although the effect of curvature is less pronounced.

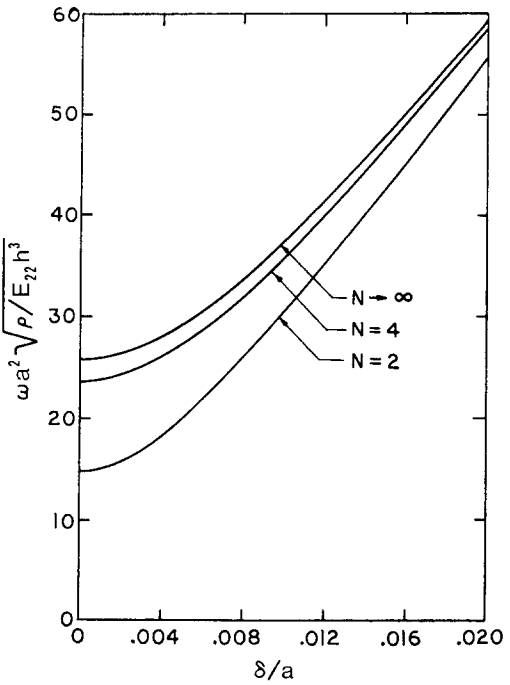

Fig. 6. Fundamental frequency as a function of initial curvature and number of layers for a square 45° angle-ply plate ($E_{11}/E_{22} = 40$, $G_{12}/E_{22} = 1$, $\nu_{12} = 0{\cdot}25$, HFT boundary condition).

REFERENCES

1. E. Reissner and Y. Stavsky, *J. Appl. Mech.* **28**, 402 (1961).
2. P. C. Yang, C. H. Norris and Y. Stavsky, *Int. J. Solids Struct.* **2**, 665 (1966).
3. J. M. Whitney and A. Leissa, *J. Appl. Mech.* **36**, 261 (1969).
4. J. M. Whitney and A. Leissa, *AIAA Jour.* **8**, 28 (1970).
5. J. M. Whitney, *J. Comp. Mat.* **4**, 192 (1970).
6. K. M. Mushtari and K. Z. Galimov, *Non-Linear Theory of Thin Elastic Shells*, p. 152. Tatkingoizdat (1957).
7. J. E. Ashton and J. M. Whitney, *Theory of Laminated Plates*. Technomic Publishing Co. (1970).
8. D. Young and R. P. Felgar, *Publication No.* 4913. University of Texas (1949).
9. C. W. Bert and B. L. Mayberry, *J. Comp. Mat.* **3**, 282 (1969).
10. J. J. Webster, *J. Int. J. Mech. Sci.* **10**, 571 (1968).
11. R. C. Fortier, Ph.D. dissertation, Northeastern University, Boston, Mass. (1972).

Абстракт — Приводится исследование поведения несимметрических слоистых анизотропных пластинок. Используя основные предположения линейной теории пластинок и зависимости для деформаций и перемещений, несколько видоизмененные в целью заключения в расчете малой начальной кривизны, даются формулы энергии и метод Ритца для получения решений статических прогибов и частот свободных колебаний. Указывается, что граничное условие с частными ограничениями в плоскости и частное размещение укладки слоев имеют важное значение на поведение пластинки, при учете сопряжения изгиба с удлиннением. Далее показывается, что малая начальная кривизна значительно повышает свободные частоты и может затемнять эффекты сопряжения изгиба с удлиннением, вследствие несимметрических слоев. Указывается также, что рост поперечной жесткости в зависимости от кривизны зависит сильно от направления волокон, ортотропии и граничных условий.

APPENDIX

The following expressions are the elements of the stiffness matrix K given by equation (13). Note that $\phi'_{wi} = \frac{\partial}{\partial t}(\phi_{wi})$, $\dot{\theta}_{wk} = \frac{\partial}{\partial t}(\theta_{wk})$, etc.

$$
\begin{aligned}
K''_{ijkl} = \int_0^a \int_0^b [&A_{11}(8\delta/a^2)^2(\phi_{wi}\phi_{wk}\theta_{wj}\theta_{wl}) \\
&- B_{11}(8\delta/a^2)(\phi_{wi}\phi''_{wk}\theta_{wj}\theta_{wl} + \phi''_{wi}\phi_{wk}\theta_{wj}\theta_{wl}) \\
&- B_{12}(8\delta/a^2)(\phi_{wi}\phi_{wk}\theta_{wj}\ddot{\theta}_{wl} + \phi_{wi}\phi_{wk}\ddot{\theta}_{wj}\theta_{wl}) \\
&- 2B_{16}(8\delta/a^2)(\phi_{wi}\phi'_{wk}\theta_{wj}\dot{\theta}_{wl} + \phi'_{wi}\phi_{wk}\dot{\theta}_{wj}\theta_{wl}) \\
&+ D_{11}(\phi''_{wi}\phi''_{wk}\theta_{wj}\theta_{wl}) \\
&+ D_{12}(\phi''_{wi}\phi_{wk}\theta_{wj}\ddot{\theta}_{wl} + \phi_{wi}\phi''_{wk}\ddot{\theta}_{wj}\theta_{wl}) \\
&+ 2D_{16}(\phi''_{wi}\phi'_{wk}\theta_{wj}\dot{\theta}_{wl} + \phi'_{wi}\phi''_{wk}\dot{\theta}_{wj}\theta_{wl}) \\
&+ D_{22}(\phi_{wi}\phi_{wk}\ddot{\theta}_{wj}\ddot{\theta}_{wl}) \\
&+ 2D_{26}(\phi_{wi}\phi'_{wk}\ddot{\theta}_{wj}\dot{\theta}_{wl} + \phi'_{wi}\phi_{wk}\dot{\theta}_{wj}\ddot{\theta}_{wl}) \\
&+ 4D_{66}(\phi'_{wi}\phi'_{wk}\dot{\theta}_{wj}\dot{\theta}_{wl})]\,dx\,dy
\end{aligned}
$$

$$
\begin{aligned}
K^{12}_{ijkl} = \int_0^a \int_0^b [&A_{11}(8\delta/a^2)(\phi'_{ui}\phi_{wk}\theta_{uj}\theta_{wl}) \\
&+ A_{16}(8\delta/a^2)(\phi_{ui}\phi_{wk}\dot{\theta}_{uj}\theta_{wl}) \\
&- B_{11}(\phi'_{ui}\phi''_{wk}\theta_{uj}\theta_{wl}) - B_{12}(\phi'_{ui}\phi_{wk}\theta_{uj}\ddot{\theta}_{wl}) \\
&- B_{16}(2\phi'_{ui}\phi'_{wk}\theta_{uj}\dot{\theta}_{wl} + \phi_{ui}\phi''_{wk}\dot{\theta}_{uj}\theta_{wl}) \\
&- B_{26}(\phi_{ui}\phi_{wk}\dot{\theta}_{uj}\ddot{\theta}_{wl}) - 2B_{66}(\phi_{ui}\phi'_{wk}\ddot{\theta}_{uj}\dot{\theta}_{wl})]\,dx\,dy
\end{aligned}
$$

$$
\begin{aligned}
K^{13}_{ijkl} = \int_0^a \int_0^b [&A_{12}(8\delta/a^2)(\phi_{vi}\phi_{wk}\dot{\theta}_{vj}\theta_{wl}) \\
&+ A_{16}(8\delta/a^2)(\phi_{vi}\phi'_{wk}\theta_{vj}\theta_{wl}) \\
&- B_{12}(\phi_{vi}\phi''_{wk}\dot{\theta}_{vj}\theta_{wl}) - B_{16}(\phi'_{vi}\phi''_{wk}\theta_{vj}\theta_{wl}) \\
&- B_{22}(\phi_{ui}\phi_{wk}\dot{\theta}_{vj}\ddot{\theta}_{wl}) \\
&- B_{26}(2\phi_{vi}\phi'_{wk}\dot{\theta}_{vj}\dot{\theta}_{wl} + \phi'_{vi}\phi_{wk}\theta_{vj}\ddot{\theta}_{wl}) \\
&- 2B_{66}(\phi'_{vi}\phi'_{wk}\theta_{vj}\dot{\theta}_{wl})]\,dx\,dy
\end{aligned}
$$

$$
\begin{aligned}
K^{22}_{ijkl} = \int_0^a \int_0^b [&A_{11}(\phi_{ui}\phi_{uk}\theta_{uj}\theta_{ul}) \\
&+ A_{16}(\phi'_{ui}\phi_{uk}\dot{\theta}_{uj}\theta_{ul} + \phi_{ui}\phi'_{uk}\dot{\theta}_{uj}\theta_{ul}) \\
&+ A_{66}(\phi_{ui}\phi_{uk}\dot{\theta}_{uj}\dot{\theta}_{ul})]\,dx\,dy
\end{aligned}
$$

$$
\begin{aligned}
K^{23}_{ijkl} = \int_0^a \int_0^b [&A_{12}(\phi_{ui}\phi'_{vk}\dot{\theta}_{uj}\theta_{vl}) \\
&+ A_{16}(\phi'_{ui}\phi'_{vk}\theta_{uj}\theta_{vl}) + A_{26}(\phi_{ui}\phi_{vk}\dot{\theta}_{uj}\dot{\theta}_{vl}) \\
&+ A_{66}(\phi'_{ui}\phi_{vk}\theta_{uj}\dot{\theta}_{vl})]\,dx\,dy
\end{aligned}
$$

$$
\begin{aligned}
K^{33}_{ijkl} = \int_0^a \int_0^b [&A_{22}(\phi_{vi}\phi_{vk}\dot{\theta}_{vj}\dot{\theta}_{vl}) \\
&+ A_{26}(\phi_{vi}\phi'_{vk}\dot{\theta}_{vj}\theta_{vl} + \phi\,\phi_{vk}{}'_{vi}\theta_{vj}\dot{\theta}_{vl}) \\
&+ A_{66}(\phi'_{vi}\phi'_{vk}\theta_{vj}\theta_{vl})]\,dx\,dy.
\end{aligned}
$$